

Structure, bonding, and reactivity of molybdenum η^3 -cyclohexenone complexes in comparison with their cyclopentenone analogues: η^3 -allyl/ η^4 -diene conversion ‡

Valentin N. Sapunov,^a Christian Slugovc,^a Kurt Mereiter,^b Roland Schmid^a and Karl Kirchner^{*†,a}

^a Institute of Inorganic Chemistry, Technical University of Vienna, Getreidemarkt 9, A-1060 Vienna, Austria

^b Institute of Mineralogy, Crystallography, and Structural Chemistry, Technical University of Vienna, Getreidemarkt 9, A-1060 Vienna, Austria

The neutral η^3 -cyclohexenone complexes [Mo(η^3 -C₆H₇O)(CO)₂(MeCN)₂Br] **1**, [Mo(η^3 -C₆H₇O)(CO)₂{HB(pz)₃}] **2**, [Mo(η^3 -C₆H₇O)(CO)₂(bipy)Br] **3** (bipy = 2,2'-bipyridine) and [Mo(η^3 -C₆H₇O)(CO)₂(dppm)Br] **4** (dppm = Ph₂PCH₂PPh₂) have been synthesized. The structure of **2** has been determined by X-ray crystallography. All these complexes resist hydride abstraction using Ph₃C⁺PF₆⁻, in sharp contrast to the η^3 -cyclopentenone analogues where η^3 -allyl/ η^4 -diene conversion is a facile process. A rationale for this different behaviour is provided by extended-Hückel calculations combined with a Walsh analysis of hydrogen abstraction. Thus, while in the η^3 -C₅H₅O → η^4 -C₅H₄O conversion a Möbius system is formed upon release of hydride *via* electrophilic attack, this is not possible in the hypothetical η^3 -C₆H₇O → η^4 -C₆H₆O process. Therefore, η^3 -C₆H₇O is a C–H acid. Also, the occurrence of different conformations, *exo* for allyl and *endo* for diene complexes, is rationalized.

Hydride abstraction from η^3 -cyclopentenone complexes of molybdenum and tungsten in [M(η^3 -C₅H₅O)(CO)₂(L₂)Br] (L₂ = bipy or dppm) and [M(η^3 -C₅H₅O)(CO)₂(L₃)] [L₃ = HB(pz)₃ or η -C₅H₅] where bipy = 2,2'-bipyridyl, dppm = bis(phosphino)methane, yields the corresponding cationic η^4 -cyclopentadienone complexes [M(η^4 -C₅H₄O)(CO)₂(L₂)Br]⁺ and [M(η^4 -C₅H₄O)(CO)₂(L₃)]⁺ (Scheme 1).^{1,2} These are reactive intermediates adding readily nucleophiles stereo- and regio-selectively to give functionalized η^3 -cyclopentenone complexes.^{3,4a} Analogous conversions have been established for a variety of η^3 -allyl (but-2-enyl, cyclohexenyl, cycloheptenyl, and cyclooctenyl) molybdenum complexes.⁴

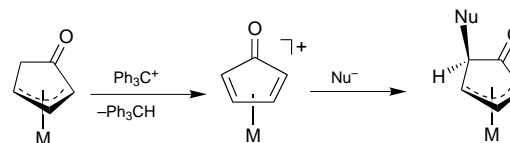
In this context it is interesting that for η^3 -cyclohexenone complexes η^3 -allyl/ η^4 -diene conversions have not been reported. In sharp contrast to the η^3 -cyclopentenone complexes, deprotonation of [Mo(C₆H₇O)(CO)₂(η -C₅H₅)] using lithium LiNPr₂ followed by treating the enolate with electrophiles leads to stereospecific alkylation at C² *anti* to the Mo(CO)₂(η -C₅H₅) group.⁵ Indeed our preliminary studies of the reactivity of [Mo(η^3 -C₆H₇O)(CO)₂{HB(pz)₃}] reveals marked differences between the chemistry of η^3 -cyclopentenone and η^3 -cyclohexenone complexes.

In this work we describe the synthesis of some molybdenum η^3 -cyclohexenone complexes as well as attempts to convert them into the cationic η^4 -C₆H₆O complexes. In addition, we provide a rationale of the differences between the cyclopentane and cyclohexane derivatives by means of extended Hückel molecular orbital (EHMO) calculations.

Experimental

General information

Manipulations were performed under an inert atmosphere of purified nitrogen or argon by using Schlenk techniques and/or a glove-box. All chemicals were standard reagent grade and used without further purification. The solvents were purified accord-



Scheme 1

ing to standard procedures.⁶ The deuterated solvents (Aldrich) were dried over 4 Å molecular sieves. Potassium tris(pyrazolyl)borate⁷ and 4-bromocyclohex-2-enone⁸ were prepared according to the literature. Proton, ³¹P-¹H} and ¹³C-¹H} NMR spectra were recorded on a Bruker AC-250 spectrometer operating at 250.13, 101.26, and 62.86 MHz, respectively, and referenced to SiMe₄ and to H₃PO₄ (85%). Diffuse reflectance Fourier-transform IR spectra were recorded on a Mattson RS 2 spectrometer.

Syntheses

[Mo(η^3 -C₆H₇O)(CO)₂(MeCN)₂Br] 1. A suspension of [Mo(CO)₆] (5.0 g, 18.94 mmol) in MeCN (15 cm³) was heated under reflux for 2 d.⁹ The resulting yellow solution containing [Mo(CO)₃(MeCN)₃] was treated at 40 °C with 4-bromocyclohex-2-enone (about 1.3-fold excess) dissolved in CCl₄ (2 cm³) for 30 min. The reaction mixture was cooled to –20 °C and an orange solid was slowly formed which was collected on a glass frit, washed with diethyl ether, and dried under vacuum. Yield: 5.88 g (76%) (Found: C, 35.41; H, 2.99; N, 6.87. C₁₂H₁₃BrMoN₂O₃ requires C, 35.23; H, 3.20; N, 6.85%). NMR [CD₃NO₂-(CD₃)₂SO (1:1), 10 °C]: δ_{H} 4.21 (br m, 1 H, allyl), 4.12 (m, 1 H, allyl), 3.91 (m, 1 H, allyl), 2.29 (m, 1 H, aliphatic), 2.04 (s, 6 H, CH₃CN), 1.95 (m, 1 H, aliphatic), 1.54 (m, 1 H, aliphatic) and 1.00 (m, 1 H, aliphatic); δ_{C} 228.4 (CO), 225.6 (CO), 200.4 (C=O), 118.2 (CH₃CN), 80.3 (allylic), 72.9 (allylic), 69.5 (allylic), 31.3 (aliphatic), 22.3 (aliphatic) and 1.0 (CH₃CN). $\tilde{\nu}_{\text{max}}/\text{cm}^{-1}$ 2312m (CN), 1969s (CO), 1887s (CO) and 1655s (C=O).

[Mo(η^3 -C₆H₇O)(CO)₂{HB(pz)₃}] 2. To a solution of compound **1** (1.34 g, 3.28 mmol) in CH₂Cl₂ (15 cm³) was added

† E-Mail: kkirch@fbch.tuwien.ac.at

‡ Non-SI unit employed: eV ≈ 1.60 × 10⁻¹⁹ J.

KHB(pz)₃ (0.83 g, 3.28 mmol) and the mixture stirred for 6 h at room temperature. The resulting precipitate of KBr was filtered off and the solvent removed under vacuum. The remaining air-stable yellow solid was purified *via* flash chromatography (neutral Al₂O₃, CH₂Cl₂ as eluent, eluting the yellow band). The volume of the solution was reduced to about 1 cm³. On addition of diethyl ether a yellow precipitate was obtained which was collected on a glass frit, washed with diethyl ether, and dried under vacuum. Yield: 1.30 g (86%) (Found: C, 44.20; H, 3.68; N, 18.10. C₁₇H₁₇BMoN₆O₃ requires C, 44.38; H, 3.72; N, 18.27%). NMR (CDCl₃, 20 °C): δ_H 8.56 [d, 1 H, *J* = 2.2, HB(pz)₃], 7.93 [d, 1 H, *J* = 2.2, HB(pz)₃], 7.72 [d, 1 H, *J* = 2.2, HB(pz)₃], 7.61 [d, 1 H, *J* = 2.2, HB(pz)₃], 7.59 [d, 1 H, *J* = 2.2, HB(pz)₃], 7.51 [d, 1 H, *J* = 2.2, HB(pz)₃], 6.29 (ppp, 1 H, *J* = 2.2, H⁴ of pz), 6.24 (p, 1 H, *J* = 2.2, H⁴ of pz), 6.18 (p, 1 H, *J* = 2.2 Hz, H⁴ of pz), 4.64–4.56 (m, 3 H, allylic), 2.61 (m, 1 H, aliphatic), 2.34 (m, 1 H, aliphatic), 1.91 (m, 1 H, aliphatic) and 1.72 (m, 1 H, aliphatic); δ_C 227.1 (CO), 224.9 (CO), 201.1 (C=O), 148.0 (pz), 145.1 (pz), 140.9 (pz), 137.0 (pz), 136.9 (pz), 135.3 (pz), 106.9 (pz), 106.38 (pz), 106.35 (pz), 79.3 (allylic), 77.9 (allylic), 66.4 (allylic), 31.3 (aliphatic) and 23.2 (aliphatic). $\tilde{\nu}_{\max}/\text{cm}^{-1}$ 2481m (BH), 1954s (CO), 1877s (CO) and 1656s (C=O).

[Mo(η^3 -C₆H₇O)(CO)₂(bipy)Br] 3. A suspension of [Mo(CO)₆] (690 mg, 2.61 mmol) in MeCN (15 cm³) was refluxed for 2 d. The resulting yellow solution was treated at 40 °C with 4-bromocyclohex-2-enone (about 1.3-fold excess) dissolved in CCl₄ (2 cm³) for 30 min. Then, a solution of bipy (408 mg, 2.61 mmol) in CH₂Cl₂ (5 cm³) was added and the mixture stirred for 30 min. After removal of the solvent the crude product was dissolved in MeCN (20 cm³). Addition of diethyl ether afforded a red microcrystalline solid which was collected on a glass frit, washed with diethyl ether, and dried under vacuum. Yield: 1.02 g (81%) (Found: C, 44.90; H, 3.20; N, 5.71. C₁₈H₁₅BrMoN₂O₃ requires C, 44.75; H, 3.13; N, 5.80%). NMR [(CD₃)₂SO, 20 °C]: δ_H 8.75–8.62 (m, 4 H, bipy), 8.23 (m, 2 H, bipy), 7.68 (m, 2 H, bipy), 4.19 (m, 1 H, allylic), 3.94 (d, 1 H, allylic), 3.80 (m, 1 H, allylic), 2.40 (m, 1 H, aliphatic), 2.10 (m, 1 H, aliphatic), 1.70 (m, 1 H, aliphatic) and 1.33 (m, 1 H, aliphatic); δ_C(45 °C) 228.4 (CO), 225.3 (CO), 199.3 (C=O), 153.3 (bipy), 151.9 (bipy), 151.8 (bipy), 139.5 (bipy), 126.4 (bipy), 123.2 (bipy), 73.4 (allylic), 68.3 (allylic), 65.2 (allylic), 30.3 (aliphatic) and 21.8 (aliphatic). $\tilde{\nu}_{\max}/\text{cm}^{-1}$ 1955s (CO), 1877s (CO) and 1654s (C=O).

[Mo(η^3 -C₆H₇O)(CO)₂(dppm)Br] 4. To a solution of compound **1** (206 mg, 0.506 mmol) in MeCN (10 cm³) was added dppm (195 mg, 0.506 mmol) and the mixture was stirred for 2 h at room temperature. The volume was reduced to about 3 cm³, whereupon an orange precipitate was formed, which was collected on a glass frit, washed with diethyl ether, and dried under vacuum. Yield: 325 mg (90%) (Found: C, 55.65; H, 4.15. C₃₃H₂₉BrMoO₃P₂ requires C, 55.72; H, 4.11%). NMR (CDCl₃, 20 °C): δ_H 7.56–7.21 (m, 20 H, dppm), 4.64 (m, 1 H, PCH₂P), 4.56–4.42 (m, 3 H, allylic), 4.01 (m, 1 H, PCH₂P), 2.46 (m, 1 H, aliphatic), 2.29 (m, 1 H, aliphatic), 1.91 (m, 1 H, aliphatic) and 1.70 (m, 1 H, aliphatic); δ_C 223 (br s, CO), 199.6 (C=O), 133.6–129.2 (dppm), 81.5 (br s, allylic), 71.0 (br s, allylic), 66.5 (br s, allylic), 35.9 (t, ¹J_{CP} = 20.6 Hz, PCH₂P), 31.2 (aliphatic) and 23.2 (aliphatic); δ_P –4.0 (br s); δ_P (–40 °C) 0.8 (d, *J*_{PP} = 8.5), 0.5 (d, *J*_{PP} = 8.5), –8.54 (d, *J*_{PP} = 8.5) and –11.64 (d, *J*_{PP} = 8.5 Hz), $\tilde{\nu}_{\max}/\text{cm}^{-1}$ 1986s (CO), 1889s (CO) and 1649s (C=O).

Reaction of compounds 2–4 with Ph₃C⁺PF₆[–]

A 5 mm NMR tube was charged with compound **2** (30 mg, 0.065 mmol) and Ph₃C⁺PF₆[–] (30 mg, 0.077 mmol) and capped with a septum. Either C₆D₆, CDCl₃, or CH₂Cl₂ (0.4 cm³) was added by syringe and the sample was transferred to a NMR probe. A ¹H NMR spectrum was immediately recorded. After

Table 1 Crystallographic data for [Mo(η^3 -C₆H₇O)(CO)₂{HB(pz)₃}]

Formula	C ₁₇ H ₁₇ BMoN ₆ O ₃
<i>M</i>	460.12
Crystal size/mm	0.12 × 0.22 × 0.73
Space group	<i>Pbca</i> (no. 61)
Crystal system	Orthorhombic
<i>a</i> /Å	19.960(3)
<i>b</i> /Å	14.190(2)
<i>c</i> /Å	13.077(2)
<i>U</i> /Å ³	3703.8(10)
<i>Z</i>	8
<i>D</i> _c /g cm ^{–3}	1.650
<i>T</i> /K	297
μ(Mo-Kα)/mm ^{–1}	0.740
Absorption correction	None
<i>F</i> (000)	1856
Minimum, maximum transmission factors	0.87–0.93
θ _{max} /°	23
Index ranges	0 ≤ <i>h</i> ≤ 23, 0 ≤ <i>k</i> ≤ 16, 0 ≤ <i>l</i> ≤ 15
No. reflections measured	3275
No. unique reflections	3275
No. observed reflections [<i>F</i> > 4σ(<i>F</i>)]	2628
No. parameters	273
<i>R</i> 1[<i>F</i> > 4σ(<i>F</i>)]	0.0283
(all data)	0.0423
<i>wR</i> 2 (all data)	0.0632
Minimum, maximum residual electron density/e Å ^{–3}	–0.269, 0.281

$R1 = \sum ||F_o| - |F_c|| / \sum |F_o|$, $wR2 = [\sum w(F_o^2 - F_c^2)^2 / \sum w(F_o^2)^2]^{1/2}$, $w = 1 / [\sigma^2(F_o^2) + (0.224P)^2 + 2.75P]$, $P = (F_o^2 + 2F_c^2) / 3$.

20 h no reaction had occurred and >97% of **2** remained. Prolonged heating at 80 °C (or in the case of chlorinated solvents at 40 °C) did not result in hydride abstraction either. The same reaction performed with **3** and **4** revealed that also no reaction took place.

X-Ray crystallography

Crystal data and experimental details for [Mo(η^3 -C₆H₇O)(CO)₂{HB(pz)₃}] **2** are given in Table 1. X-Ray data were collected on a Philips PW1100 four-circle diffractometer using graphite-monochromated Mo-Kα (λ = 0.71069 Å) radiation and the θ–2θ scan technique. Three representative reference reflections were measured every 120 min and used to correct for crystal decay and system instability. Corrections for Lorentz-polarization effects were applied. The structure was solved by direct methods.¹⁰ All non-hydrogen atoms were refined anisotropically, and hydrogen atoms were included in idealized positions.¹¹ The structure was refined against *F*².

CCDC reference number 186/651.

Extended Hückel molecular orbital calculations

The EHMO calculations were conducted by using the program developed by Hoffmann and Lipscomb,¹² and modified by Mealli and Proserpio.¹³ The atomic orbital (AO) parameters used were taken from the CACAO program.¹³

Results and Discussion

The compound [Mo(CO)₃(MeCN)₃], prepared *in situ* by refluxing [Mo(CO)₆] in MeCN, reacts with 4-bromocyclohex-2-enone to afford the neutral η^3 -cyclohexenone complex [Mo(η^3 -C₆H₇O)(CO)₂(MeCN)₂Br] **1** in 76% isolated yield. Conversion into complexes [Mo(η^3 -C₆H₇O)(CO)₂{HB(pz)₃}] **2**, [Mo(η^3 -C₆H₇O)(CO)₂(bipy)Br] **3** and [Mo(η^3 -C₆H₇O)(CO)₂(dppm)Br] **4** was accomplished by treatment of **1** with stoichiometric amounts of either KHB(pz)₃, bipy, or dppm in CH₂Cl₂ or MeCN as the solvents. All compounds are crystalline solids ranging from yellow to red. They are generally air-stable

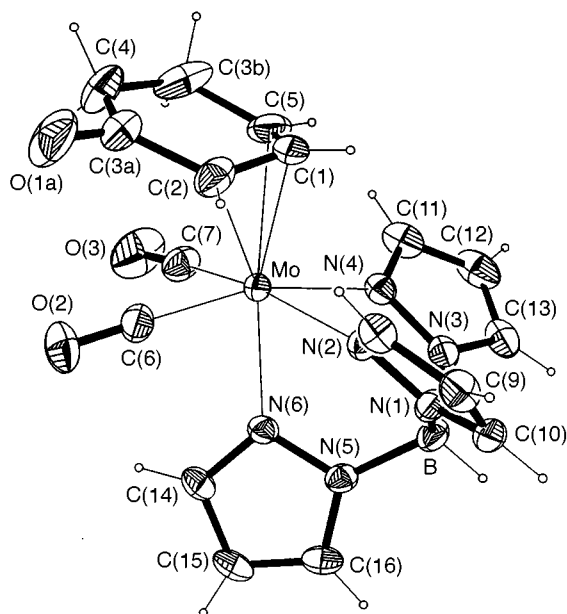


Fig. 1 Structural view of $[\text{Mo}(\eta^3\text{-C}_6\text{H}_7\text{O})(\text{CO})_2\{\text{HB}(\text{pz})_3\}]$ **2** showing 30% probability thermal ellipsoids. Selected bond lengths (Å) and angles ($^\circ$): Mo–C(1) 2.206(3), Mo–C(2) 2.354(4), Mo–C(5) 2.364(3), Mo–C(6) 1.957(3), Mo–C(7) 1.941(3), Mo–N(2) 2.291(2), Mo–N(4) 2.268(3), Mo–N(6) 2.192(2), C(1)–C(2) 1.379(5) and C(1)–C(5) 1.373(6); C(5)–C(1)–C(2) 116.0(4), C(6)–Mo–N(6) 83.9(1), C(6)–Mo–N(4) 161.6(1) and C(6)–Mo–N(2) 100.1(1)

in the solid state and also for extended periods in solution. Complexes **1–4** have been fully characterized by a combination of elemental analysis, IR, ^1H , and $^{13}\text{C}\text{-}\{^1\text{H}\}$ NMR spectroscopy, and by $^{31}\text{P}\text{-}\{^1\text{H}\}$ NMR spectroscopy for **4**.

The IR spectra of complexes **1–4** display the expected absorptions for a *cis* dicarbonyl structure in the ranges 1969–1951 and 1889–1857 cm^{-1} , respectively, similar to those of the analogous cyclopentenone complexes reported previously.¹ The C=O stretching frequency of the ketonic carbonyl of the cyclohexenone ligand is found in the range 1656–1649 cm^{-1} .

The ^1H NMR spectra of complexes **1–3** show the expected resonances for the cyclopentenone moiety giving rise to three multiplets for the allyl protons and four for the aliphatic protons. All aliphatic protons (H_{syn} and H_{anti}) are clearly separated. The coligands MeCN, $\text{HB}(\text{pz})_3$, and bipy exhibit resonances in the usual ranges. The $^{13}\text{C}\text{-}\{^1\text{H}\}$ NMR spectra bear no unusual features with the characteristic resonances of the ketonic carbonyl carbon observed at δ 200.4, 201.1, and 199.3, respectively. The *cis* carbonyl ligands are magnetically inequivalent, giving rise to resonances at δ 228.4 and 225.6, 227.1 and 224.9, and 228.4 and 225.3, respectively. This is also expected on the basis of the IR data since **1–3** apparently do not contain a plane of symmetry.

The ^1H , $^{13}\text{C}\text{-}\{^1\text{H}\}$ and $^{31}\text{P}\text{-}\{^1\text{H}\}$ NMR spectra of complex **4** reveal that it is fluxional at room temperature leading to broadened resonances. The fluxional behaviour is likely due to an equilibrium between *exo* and *endo* isomers¹⁴ and/or a trigonal twist rearrangement.¹⁵ Most informative is the $^{31}\text{P}\text{-}\{^1\text{H}\}$ NMR spectrum of **4**. At room temperature it exhibits only a broad signal at δ –4. However, on lowering the temperature of the NMR probe to –40 $^\circ\text{C}$ two pairs of doublets centred at δ 0.8 ($J_{\text{PP}} = 8.5$) and –11.64 ($J_{\text{PP}} = 8.5$) and 0.5 ($J_{\text{PP}} = 8.5$) and –8.54 ($J_{\text{PP}} = 8.5$ Hz) are observed (*ca.* 3:2 ratio) suggesting the presence of *exo* and *endo* isomers. Similar observations have been made for other molybdenum and tungsten complexes of the types $[\text{M}(\eta^3\text{-C}_5\text{H}_5\text{O})(\text{CO})_2(\text{L}_2)\text{Br}]$ and $[\text{M}(\eta^3\text{-C}_5\text{H}_5\text{O})(\text{CO})_2(\text{L}_3)]$ with the *exo* isomer being the predominant species.^{14,16} A rationalization of the rotational preference of the η^3 -allyl group based on EHMO calculations has been given previously.¹⁷ A

low-temperature $^{13}\text{C}\text{-}\{^1\text{H}\}$ NMR spectrum was precluded due to the poor solubility of **4**.

The structure of complex **2**, as determined by X-ray crystallography, is shown in Fig. 1 with selected bond lengths and angles reported in the caption. Thus, **2** is pseudo-octahedral with the η^3 -cyclohexenone moiety occupying one co-ordination site. An equatorial plane can be defined to include the two carbonyls [C(6) and C(7)] and two nitrogen atoms [N(2), N(4)] of the $\text{HB}(\text{pz})_3$ ligand. The η^3 -cyclohexenone ligand and the third nitrogen atom [N(6)] of the $\text{HB}(\text{pz})_3$ ligand lie *trans* to one another in apical positions above and below the equatorial plane. The η^3 -cyclohexenone moiety adopts exclusively the *exo* conformation with respect to the orientation of the allyl moiety. In fact this conformation is found for all complexes featuring the $\text{M}(\eta^3\text{-allyl})(\text{CO})_2$ moiety (M = Mo or W) the structures of which have been determined and thus appears to be a general trend.^{1–5,15,16} The η^3 -cyclohexenone moiety is distinctly bent and can be subdivided by two planes. The plane defined by C(1), C(2), and C(5) (allyl fragment) forms an angle of 31.2(3) $^\circ$ with that defined by C(3a), C(3b), C(4) and C(5). The η^3 -cyclohexenone ligand exhibits a disorder of the ketonic oxygen being attached either to the C(3a) or to the C(3b) atom in a 2:1 ratio. The Mo–CO and C–O distances are both within the ranges reported for other molybdenum carbonyl complexes. There are no structural features indicating unusual deviations or distortions. The complex $[\text{Mo}(\eta^3\text{-C}_6\text{H}_7\text{O})(\text{CO})_2\{\text{HB}(\text{pz})_3\}]$ is practically isostructural with $[\text{Mo}(\eta^3\text{-C}_5\text{H}_5\text{O})(\text{CO})_2\{\text{HB}(\text{pz})_3\}]$.¹

Reaction of complexes **2–4** with $\text{Ph}_3\text{C}^+\text{PF}_6^-$

Treatment of complexes **2–4** with $\text{Ph}_3\text{C}^+\text{PF}_6^-$ in either C_6D_6 , CD_2Cl_2 , or CDCl_3 did not result in hydride abstraction even after prolonged heating as monitored by ^1H NMR spectroscopy. Only traces of Ph_3COH were detected presumably formed from residual water of the solvents.

EHMO calculations

It thus appears to be substantiated that η^3 -cyclohexenone complexes do not undergo an η^3 -allyl/ η^4 -diene conversion in marked contrast to the η^3 -cyclopentenone analogues. In attempting to provide some rationale for this difference EHMO calculations have been performed considering the $\text{M}(\text{CO})_2\text{-}\{\text{HB}(\text{pz})_3\}^+$ fragment and its bonding mode to a sixth ligand following the work of Curtis *et al.*¹⁸ and ours.¹⁹

$\text{Mo}(\text{CO})_2\{\text{HB}(\text{pz})_3\}^+$. For the σ – σ interactions, the highest $d(\sigma^*)$ orbital ($\Psi_{1\text{Mo}}$, ‘classical’ $d_{x^2-y^2}$, $E = -4.68$ eV) is typical of σ – σ interactions in square-pyramidal complexes, using three sp^2 and two sp hybrid electron pairs of N and CO, respectively, without π participation of the ligands. The energy of $\Psi_{1\text{Mo}}$ remains virtually unchanged when the sixth ligand enters. The other $d(\sigma^*)$ orbital ($\Psi_{2\text{Mo}}$, ‘classical’ d_z^* , $E = -9.36$ eV) is, by contrast, slightly affected by the π^* MOs of the two CO ligands. This orbital is located primarily in the z direction perpendicular to the pyramidal base and is responsible for the σ -acceptor property of the fragment. In the case of η^3 -allyl or η^4 -diene, these ligands form a σ bond by interacting with d_z^* (decrease in energy of d_z^* from –9.36 to –4.50 eV) and π_{sym} -MO of the allyl or diene moiety.

For the π – π interactions, the three d_{xy} , d_{xz} and d_{yz} AOs of Mo interact with the appropriate π^* orbitals of the COs, but without participation of π [$\text{HB}(\text{pz})_3$], giving the new orbitals d_{xy}' , d_{xz}' and d_{yz}' , with the greatest overlap population (31) calculated for d_{xy}' . Whereas d_{xy}' lies in the basal plane (xy) of the pyramid orbital and is not affected by the sixth ligand, the two others are arranged in the xz and yz planes. In the case of an idealized structure of $\text{Mo}(\text{CO})_2\{\text{HB}(\text{pz})_3\}^+$ (*i.e.* equal Mo–N and Mo–C bond lengths and an O–C–Mo angle of 180 $^\circ$), the two d_{xz}' and d_{yz}' orbitals form new π -type hybrids ($h_1 = d_{xz}' - d_{yz}'$ and $h_2 = d_{xz}' + d_{yz}'$), with splittings –10.86 and

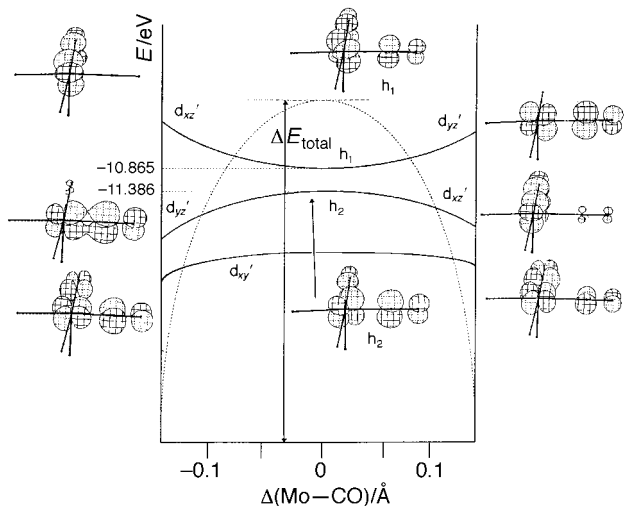


Fig. 2 Effect of asymmetric oscillation of the CO ligands on the energy and geometry of the t_{2g} set of the $\text{Mo}(\text{CO})_2\{\text{HB}(\text{pz})_3\}$ fragment. On the abscissa are shown the differences between two Mo–CO bond lengths

–11.39 eV. However, if the structure is even slightly distorted, rehybridization into d_{xz}' and d_{yz}' takes place. This effect was not investigated by Curtis and Eisenstein.¹⁷ Actually, the d_{xz}' and d_{yz}' or h_1 and h_2 orbitals may be considered as limiting cases.

Thus, rotation of the CO molecule about the Mo–C–O axis does not change the geometry of h_1 and h_2 , while a small difference between the two Mo–CO bonds due to asymmetric oscillations of the CO ligands makes h_1 and h_2 transform into d_{xz}' and d_{yz}' . According to a Walsh diagram, the maximum energy (minimum stabilization) of the $\text{Mo}(\text{CO})_2\{\text{HB}(\text{pz})_3\}$ moiety occurs when the two Mo–CO bond lengths are equal (Fig. 2). The asymmetric oscillation of the two CO ligands affords stabilization by about 0.15 eV for a 0.1 Å change in distance. It would appear that the inequivalence of the two CO ligands, as reflected by different C–O stretching frequencies, is an important diagnostic for the state of hybridization of the $d(\pi)$ orbitals (see below). Owing to the low $d_{xz,yz}' \leftrightarrow h_{1,2}$ rehybridization energy, the sixth ligand can provoke the one orbital geometry or the other, depending on the π -acceptor or -donor property of the ligand. In the case of d^4 Mo, the $d(\pi)$ orbitals accommodate two electrons and can serve as either π acceptor or π donor.

$\text{Mo}(\text{CO})_2\{\text{HB}(\text{pz})_3\}\text{L}$. The co-ordination geometry of the sixth ligand L depends much on the degree of filling of the active $d(\pi)$ orbitals (d_{xz}' and d_{yz}' or h_1 and h_2), which can act as either a π acceptor or π donor towards the diene or allyl ligand orbitals of appropriate symmetry. Both η^4 -diene and η^3 -allyl planes are coplanar with the base of the square pyramid for optimum π overlap to be attained.

In all known crystal structures the co-ordinated η^3 -allyl group is found to adopt the *exo* conformation, *i.e.* its open face is placed toward the adjacent two carbonyls, whereas the $\text{C}_5\text{H}_4\text{O}$ ligand prefers the *endo* orientation. Both these characteristics are correctly reproduced by a Walsh analysis. Thus, the rotation of the allyl fragment about the σ bond has two minima for the *exo* and *endo* conformations with the former preferred by about 0.2 eV for η^3 - $\text{C}_5\text{H}_5\text{O}$ and 0.4 eV for η^3 - $\text{C}_6\text{H}_7\text{O}$ (*cf.* ref. 17). Likewise, the rotation of $\text{C}_5\text{H}_4\text{O}$ involves two minima, but now the *endo* conformation is somewhat more stable (0.1 eV) than the *exo* conformation. In contrast, for the hypothetical $\text{C}_6\text{H}_6\text{O}$ ligand the *exo* orientation is calculated to be *ca.* 0.5 eV more stable over an *endo* arrangement. Common to all rotations analysed here is the high barrier (η^3 - $\text{C}_5\text{H}_5\text{O}$, 1.0; η^3 - $\text{C}_6\text{H}_7\text{O}$, 1.5; $\text{C}_5\text{H}_4\text{O}$, 1.2; $\text{C}_6\text{H}_6\text{O}$, 3.6 eV). Noteworthy, these rotation barriers are of the order of the total stabilization energies of the sixth ligand, except for $\text{C}_6\text{H}_6\text{O}$ which is much less

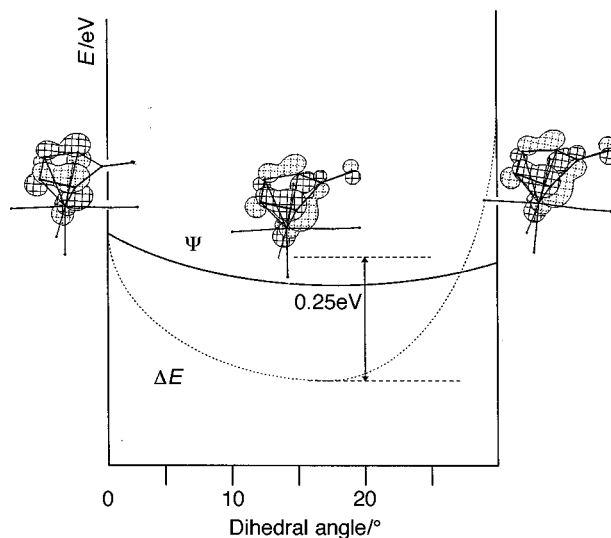


Fig. 3 Variation in overlap between π_{asym} (LUMO of the $\text{C}_5\text{H}_4\text{O}$) and the fragment h_1 hybrid of $[\text{Mo}(\eta^4\text{-C}_5\text{H}_4\text{O})(\text{CO})_2\{\text{HB}(\text{pz})_3\}]^+$ with the dihedral angle between dienic and $\text{CHC}(\text{O})\text{CH}$ planes (formation of a Möbius orbital). Shown is (—) the bonding π MO (Ψ) and (....) the total energy (ΔE) of the complex varying with the conformation of $\text{C}_5\text{H}_4\text{O}$ from planar to bent

stabilized (only *ca.* 0.1 eV). Such high barriers compared to the total stabilization energies imply a non-flexible structure of the active $d(\pi)$ orbitals and that the π and not the σ interactions are the decisive factor in the rotational preference.

$\text{C}_5\text{H}_4\text{O}$ vs. $\text{C}_6\text{H}_6\text{O}$. The conformations of $[\text{Mo}(\eta^4\text{-C}_5\text{H}_4\text{O})(\text{CO})_2\{\text{HB}(\text{pz})_3\}]^+$ and the hypothetical $\text{C}_6\text{H}_6\text{O}$ variant $[\text{Mo}(\eta^4\text{-C}_6\text{H}_6\text{O})(\text{CO})_2\{\text{HB}(\text{pz})_3\}]^+$ (for structure adoption see Appendix) are determined by forming bonds through overlap of h_1 (lowest unoccupied molecular orbital, LUMO) and h_2 (highest unoccupied molecular orbital, HOMO) of the molybdenum fragment and π_{asym} (HOMO, as the donor) and π^*_{asym} (LUMO, as the acceptor) of the dienone. In the $\text{C}_5\text{H}_4\text{O}$ case the two π interactions $\text{M} \rightarrow \text{L}$ and $\text{M} \leftarrow \text{L}$ are equivocally effective (overlap populations 21 and 26) whereas for $\text{C}_6\text{H}_6\text{O}$ both are weak (overlap populations 2 and 5). The favourable overlap for $\text{C}_6\text{H}_6\text{O}$ of (unoccupied) h_1 with π^*_{asym} (LUMO) (overlap population = 20) and (occupied) h_2 with π_{asym} (HOMO) (overlap population = 18) is not effective, of course. Thus, the difference between the two dienone complexes rests on the different symmetries of the active orbitals. Relevant to the issue is the finding that in all known $\text{C}_5\text{H}_4\text{O}$ complexes, independent of the metal, a dihedral angle of 15 to 25° is observed between the planes of the C_4 -diene fragment and the $\text{C}_\alpha\text{C}(\text{=O})\text{C}_\alpha'$ atoms.^{1,20} This result is well reproduced by a Walsh analysis. While the free $\text{C}_5\text{H}_4\text{O}$ molecule is most stable in the planar form indeed, for $[\text{Mo}(\eta^4\text{-C}_5\text{H}_4\text{O})(\text{CO})_2\{\text{HB}(\text{pz})_3\}]^+$ there is an increase in energy by 0.2–0.3 eV for a 20° dihedral angle. The reason is that a bent $\text{C}_5\text{H}_4\text{O}$ ring experiences better overlap of its π_{asym} (LUMO) and π^*_{asym} (HOMO) with the $d(\pi)$ hybrid MO of the fragment because of shift in electron density from terminal C_α and C_α' to central C_β and C_β' , with the creation of a Möbius system (Fig. 3). No such possibility exists for a $\text{C}_6\text{H}_6\text{O}$ complex.

η^3 - $\text{C}_5\text{H}_5\text{O}$ vs. η^3 - $\text{C}_6\text{H}_7\text{O}$. For the case of the parent allyl group C_3H_5 there is already the MO analysis of Curtis and Eisenstein,¹⁷ according to which the preference of the *exo* conformation of the allyl moiety results from a second-order mixing of σ - and π -type orbitals on the metal through the CO π^* orbitals. In our case, the presence of a ketonic carbonyl adjacent to allyl changes noticeably the geometry of the active orbitals. An important contribution to the complex stability derives from the overlap of the unoccupied distorted h_1 (practically d_{xz}') of the Mo and π_{asym} (HOMO, or 'classical' n) of

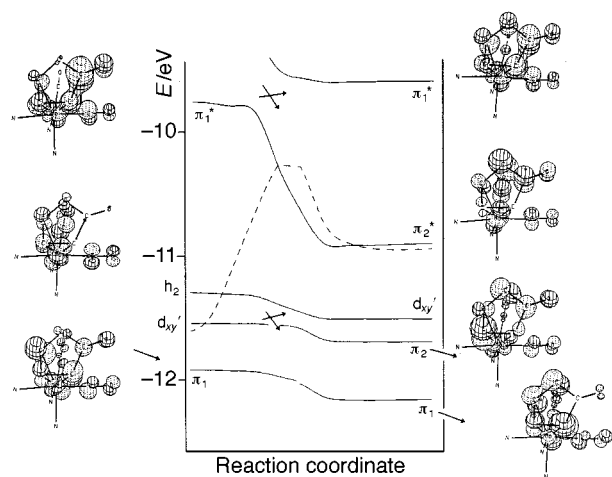
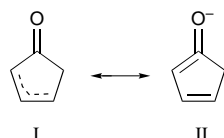


Fig. 4 Walsh diagram for hydrogen abstraction in the $[\text{Mo}(\text{CO})_2(\eta^3\text{-C}_5\text{H}_5\text{O})\{\text{HB}(\text{pz})_3\}] \longrightarrow [\text{Mo}(\text{CO})_2(\eta^3\text{-C}_5\text{H}_4\text{O})\{\text{HB}(\text{pz})_3\}]^+$ transformation without geometry optimization. The fragment MO (FMO) d_{xy}' remains unchanged in the fragment and complex; π_1/π_1^* and π_2/π_2^* show the π - $d(\pi)$ overlap between $\text{Mo}(\text{CO})_2\{\text{HB}(\text{pz})_3\}$ and $\eta^3\text{-C}_5\text{H}_5\text{O}$ or $\eta^3\text{-C}_5\text{H}_4\text{O}$ ligand. The broken line represents the potential energy surface (see text)



$\text{C}_5\text{H}_5\text{O}$ or $\text{C}_6\text{H}_7\text{O}$ (overlap populations of 20 or 23, respectively), forming the $\text{M} \leftarrow \text{L}$ bond. The HOMO of $\eta^3\text{-C}_5\text{H}_5\text{O}$ and $\eta^3\text{-C}_6\text{H}_7\text{O}$ includes the conjugation between the p-electron pair of the allyl fragment **I** and π^* of the ketonic CO leading to the pseudo-diene configuration **II** that finds its symmetry match in the h_1 hybrid.

Therefore, the present *exo* orientation preference is even reinforced compared to that of the parent allyl ligand. This type of bonding is realized in several $[\text{Mo}(\eta^3\text{-}\gamma\text{-lactonyl})(\text{CO})_2(\eta^3\text{-C}_5\text{H}_5)]$ complexes.²¹ Incidentally, the active π orbital (h_2 , occupied) of the $\text{Mo}(\text{CO})_2\{\text{HB}(\text{pz})_3\}$ moiety is little affected by co-ordination to allyl because π^* (LUMO) of the latter only slightly contributes to the complex stability. The respective overlap populations of 8 for $\text{C}_5\text{H}_5\text{O}$ and 7 for $\text{C}_6\text{H}_7\text{O}$ indicate the absence of appreciable $\text{M} \rightarrow \text{L}$ interactions. On the other hand, the interaction of π^* (LUMO) of allyl with h_2 is localized onto the allyl C_m rendering appreciable σ character. Summed up, there is not much difference in bonding between $[\text{Mo}(\eta^3\text{-C}_5\text{H}_5\text{O})(\text{CO})_2\{\text{HB}(\text{pz})_3\}]$ and $[\text{Mo}(\eta^3\text{-C}_6\text{H}_7\text{O})(\text{CO})_2\{\text{HB}(\text{pz})_3\}]$ in sharp contrast to the diene analogues above.

The theoretical analysis is supplemented by the variation in the physicochemical properties of the CO ligands reflected in the CO stretching frequencies. As is well known, the change in vibrational frequency for a bond is diagnostic of the change in force constant for the bond or as a probe of the electronic structure of a series of compounds. From group theory it is predicted that the present complexes (roughly C_{2v}) should exhibit two infrared-active CO stretching vibrations a_1 and b_2 . For the diene complexes, two bands at about 2090 and 2030 cm^{-1} , and for the allyl complexes two bands at about 1990 and 1890 cm^{-1} are observed (or about 1990 and 1920 cm^{-1} for allyl ligands like $\eta^3\text{-C}_5\text{H}_4\text{O}(\text{PR}_3)_5$). Thus, the symmetric vibration mode a_1 decreases by 100 cm^{-1} (from 2090 to 1990 cm^{-1}) in going from the diene to the allyl complexes. This is in agreement with the classical rule²² that a unit of negative charge, or decrease in oxidation state of the metal, lowers $\nu(\text{CO})$ by about 100 cm^{-1} due to more $\text{M} \rightarrow (\pi^*)\text{CO}$ back donation. In the present case the electronic charge of the donor orbital of the sixth ligand (neutral for diene and negative for allyl) is relevant. Simi-

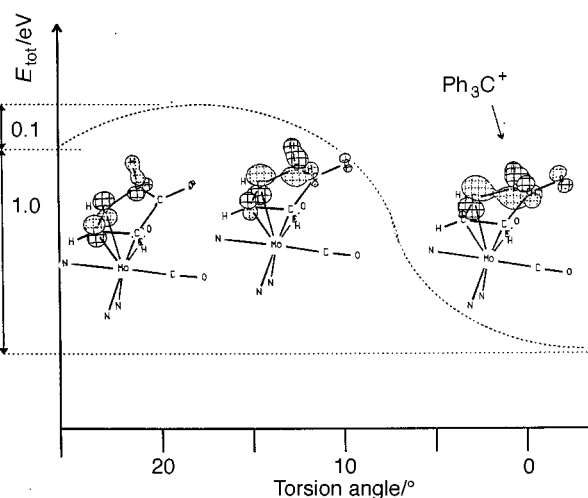


Fig. 5 Variable participation of the AO of H in the allylic fragment of the HOMO of the $[\text{Mo}(\eta^3\text{-C}_5\text{H}_5\text{O})(\text{CO})_2\{\text{HB}(\text{pz})_3\}]$ complex upon *gauche* deformation of the methylenic group as a condition for Ph_3C^+ cationic attack at the H atom. The abscissa gives the change in the torsion angle between the allylic fragment and the carbon atom of the methylenic group

larly, the asymmetric vibration level b_1 decreases from 2030 to 1920 [or about 1890 cm^{-1} for allyl ligands like $\eta^3\text{-C}_5\text{H}_4\text{O}(\text{PR}_3)_5$]. The difference between the a_1 and b_2 bands is likely related to the energy of $\text{C}^+\text{O}^{\delta-}$ dipole formation in the effective charge field of the complex (electronic-vibrational coupling).²³

η^3 -Allyl/ η^4 -diene conversion. The above MO analysis combined with a Walsh analysis of hydrogen abstraction (Fig. 4) in the $\eta^3\text{-C}_5\text{H}_5\text{O} \longrightarrow \eta^4\text{-C}_5\text{H}_4\text{O}$ transformation shows a new energetically favourable $\text{M} \rightarrow \text{L}$ interaction arising provided the hydrogen is released as hydride. Otherwise two electrons would remain in the new antibonding orbital destabilizing this new interaction. In the HOMO of the $\eta^3\text{-C}_5\text{H}_5\text{O}$ complex the AO of the H to be released is participating. This contribution is increased in the case of a *gauche* deformation of the methylene group similar to the transition state for nucleophilic attack at the $\text{C}_5\text{H}_4\text{O}$ ligand described previously.²⁴ Therefore, electrophilic attack can be expected to occur at this H atom. The computer simulation of Ph_3C^+ attack at the H atom with simultaneous hydrogen abstraction (but without geometry optimization of the product) reveals that the HOMO is lowered in energy by 1.0 eV with a small activation barrier of *ca.* 0.1 eV (Fig. 5). Interestingly, the same simulation at uncomplexed allyl gives a high barrier (1.2–1.4 eV) for hydride abstraction, revealing the importance of the back bonding to the stability of the diene complex formed. On the other hand, attack of Ph_3C^+ at the O atom, not involved in the HOMO of the $\eta^3\text{-C}_5\text{H}_5\text{O}$ complex, is not effective.

In contrast, in the $\eta^3\text{-C}_6\text{H}_7\text{O} \longrightarrow \eta^4\text{-C}_6\text{H}_6\text{O}$ conversion (Fig. 6) no $\text{M} \rightarrow \text{L}$ interaction is involved (h_2 is only slightly stabilized from -11.11 to -11.18 eV). The new orbital (-10.5 eV, HOMO) is virtually a p orbital of a non-allyl carbon. This is typical of a C–H acid such as chloroform (the energy level of the HOMO of the CCl_3^- anion is calculated to be -10.6 eV). This is in line with the ease of deuteration of $\eta^3\text{-C}_6\text{H}_7\text{O}$ molybdenum complexes in basic media.⁵ In contrast to the $\eta^3\text{-C}_5\text{H}_5\text{O}$ complex, in the HOMO of the $\eta^3\text{-C}_6\text{H}_7\text{O}$ complex the AO of O is participating. However, the attack of Ph_3C^+ at the O atom appears to be unfavourable on steric grounds.

Appendix

The structure of the hypothetical diene complex $[\text{Mo}(\eta^4\text{-C}_6\text{H}_6\text{O})(\text{CO})_2\{\text{HB}(\text{pz})_3\}]^+$ was approximated from the crystal structure of the $\text{C}_5\text{H}_4\text{O}$ analogue. Both the $\text{Mo} \rightarrow \text{L}$ distance and

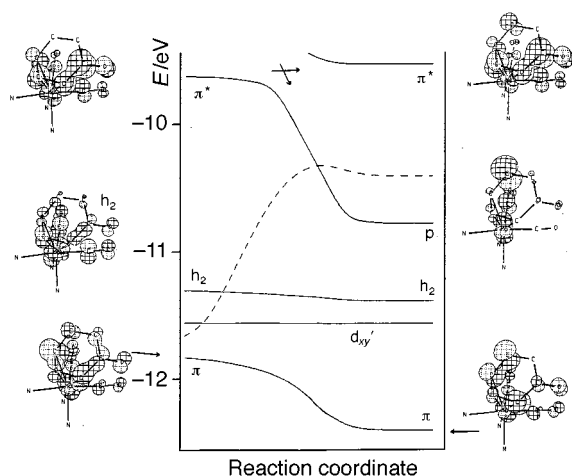


Fig. 6 Walsh diagram for hydrogen abstraction in the transformation $[\text{Mo}(\eta^3\text{-C}_6\text{H}_7\text{O})(\text{CO})_2\{\text{HB}(\text{pz})_3\}] \longrightarrow [\text{Mo}(\eta^4\text{-C}_6\text{H}_6\text{O})(\text{CO})_2\{\text{HB}(\text{pz})_3\}]^+$ without geometry optimization. The orbitals d_{xy} and h_2 are the invariant FMOs in the initial complex and the product; π/π^* shows the π - $d(\pi)$ overlap between $\text{Mo}(\text{CO})_2\{\text{HB}(\text{pz})_3\}$ and $\eta^3\text{-C}_6\text{H}_7\text{O}$ or $\eta^3\text{-C}_6\text{H}_6\text{O}$ ligand. The broken line represents the potential energy surface

the torsion angle between the diene and the $\text{CHCH}_2\text{C}(=\text{O})\text{CH}$ planes were optimized. The resulting dihedral angle equal to $\approx 30^\circ$ is in agreement with other calculations.²⁵ Since the equilibrium geometry of phenol is proposed to be about 2.0 eV lower in energy than that of cyclohexa-2,4-dien-1-one (planar),²⁶ the stabilization energy of the $\text{C}_6\text{H}_6\text{O}$ complex should exceed this value. This is possible, if the π acceptor orbital of the metal fragment is lower in energy than the HOMO of $\text{C}_6\text{H}_6\text{O}$ (-11.80 eV), as in the ruthenium complex [$\Psi(d) = -12.2$ eV]. The tautomerization of $[\text{Ru}^0(\eta^6\text{-C}_6\text{H}_6)(\eta^4\text{-C}_6\text{H}_6\text{O})]$ into $[\text{Ru}^0(\eta^6\text{-C}_6\text{H}_6)(\eta^6\text{-C}_6\text{H}_5\text{OH})]$ is completely repressed.²⁷

Acknowledgements

Financial support by the Fonds zur Förderung der wissenschaftlichen Forschung in Österreich is gratefully acknowledged (Projekt 11896-CHE).

References

- 1 K. Mauthner, C. Slugovc, K. Mereiter, R. Schmid and K. Kirchner, *Organometallics*, 1996, **15**, 181.
- 2 A. Rubio and L. S. Liebeskind, *J. Am. Chem. Soc.*, 1993, **115**, 891.
- 3 C. Slugovc, K. Mauthner, K. Mereiter, R. Schmid and K. Kirchner, *Organometallics*, 1996, **15**, 2954.
- 4 (a) J. Ipaktschi and A. J. Hartmann, *J. Organomet. Chem.*, 1992, **431**, 303; (b) J. Ipaktschi and A. J. Hartmann, *J. Organomet. Chem.*, 1992,

- 434, 303; (c) A. J. Pearson, Md. N. I. Khan, J. C. Clardy and He Cun-Heng, *J. Am. Chem. Soc.*, 1985, **107**, 2748.
- 5 A. J. Pearson, S. Mallik, R. Motezaei, M. W. D. Perry, R. J. Shively and W. J. Youngs, *J. Am. Chem. Soc.*, 1990, **112**, 8034.
- 6 D. D. Perrin and W. L. F. Armarego, *Purification of Laboratory Chemicals*, 3rd edn., Pergamon, New York, 1988.
- 7 S. Trofimenko, *Inorg. Synth.*, 1970, **12**, 99.
- 8 C. H. Depuy, M. Isaks, K. L. Eilers and G. F. Morris, *J. Org. Chem.*, 1964, **20**, 3503.
- 9 D. P. Tate, W. R. Knipple and J. M. Aufl, *Inorg. Chem.*, 1962, **1**, 433; G. J. Kubas and L. S. van der Sluys, *Inorg. Synth.*, 1990, **28**, 29.
- 10 S. R. Hall, H. D. Flack and J. M. Stewart, XTAL3.2, Integrated system of computer programs for crystal structure determination, Universities of Western Australia (Australia), Geneva (Switzerland) and Maryland (USA), 1992.
- 11 G. M. Sheldrick, SHELXL 93, Program for crystal structure refinement, University of Göttingen, 1993.
- 12 R. Hoffmann and W. N. Liscomb, *J. Chem. Phys.*, 1962, **36**, 2179, 3489; R. Hoffmann, *J. Chem. Phys.*, 1963, **39**, 1397.
- 13 C. Mealli and D. M. Proserpio, *J. Chem. Educ.*, 1990, **67**, 399.
- 14 L. S. Liebeskind and A. Bombrun, *J. Am. Chem. Soc.*, 1991, **113**, 8736.
- 15 J. W. Faller, D. A. Haitko, R. D. Adams and D. F. J. Chodosh, *J. Am. Chem. Soc.*, 1979, **101**, 865.
- 16 S. Hansson, J. F. Miller and L. S. Liebeskind, *J. Am. Chem. Soc.*, 1990, **112**, 9660; A. J. Pearson, S. Malik, A. A. Pinkerton, J. P. Adams and S. Zheng, *J. Org. Chem.*, 1992, **57**, 2910; A. J. Pearson, S. L. Blystone, H. Nar, A. A. Pinkerton, B. A. Roden and J. Yoon, *J. Am. Chem. Soc.*, 1989, **111**, 134; A. J. Pearson, M. N. I. Khan, J. C. Clardy and H. Ciu-Heng, *J. Am. Chem. Soc.*, 1985, **107**, 2748; J. W. Faller, H. H. Murray, D. L. White and K. H. Chao, *Organometallics*, 1983, **2**, 400; Y. D. Ward, L. A. Villanueva, G. D. Allred, S. C. Payne, M. A. Semones and L. S. Liebeskind, *Organometallics* 1995, **14**, 4132.
- 17 M. D. Curtis and O. Eisenstein, *Organometallics*, 1984, **3**, 887.
- 18 M. D. Curtis and K.-B. Shiu, *Inorg. Chem.*, 1985, **24**, 1213; M. D. Curtis, K. S. B. Shiu, W. M. Butler and J. C. Huffman, *J. Am. Chem. Soc.*, 1986, **108**, 3335.
- 19 C. Gemel, P. Wiede, K. Mereiter, V. N. Sapunov, R. Schmid and K. Kirchner, *J. Chem. Soc., Dalton Trans.*, 1996, 4071; G. Trimmel, C. Slugovc, P. Wiede, K. Mereiter, V. N. Sapunov, R. Schmid and K. Kirchner, *Inorg. Chem.*, 1997, **36**, 1076.
- 20 K. Kirchner, K. Mereiter, A. Umfahrer and R. Schmid, *Organometallics*, 1994, **13**, 1886.
- 21 C. Butters, N. Carr, R. J. Deeth, M. Green, S. M. Green and M. F. Mahon, *J. Chem. Soc., Dalton Trans.*, 1996, 2299.
- 22 F. Basolo and R. G. Pearson, *Mechanisms of Inorganic Reactions*, 2nd edn., Wiley, New York, 1967, p. 536.
- 23 K. G. Spears, X. Wen and R. Zhang, *J. Phys. Chem.*, 1996, **100**, 10206.
- 24 C. Gemel, D. Kalt, K. Mereiter, V. N. Sapunov, R. Schmid and K. Kirchner, *Organometallics*, 1997, **16**, 427.
- 25 O. V. Shishkin and Y. T. Strukov, *Russ. Chem. Bull.*, 1995, **44**, 823.
- 26 K. Mandix, *Int. J. Quantum Chem.*, 1993, **46**, 159.
- 27 N. Oshima, H. Suzuki and Y. Moro-oka, *Inorg. Chem.*, 1986, **25**, 3407.

Received 27th May 1997; Paper 7/03633G